DEUTSCHES ELEKTRONEN-SYNCHROTRON DESY

DESY 82-047
July 1982

HADRONIC FINAL STATES IN HIGH ENERGY MUON-NUCLEON SCATTERING, RECENT RESULTS FROM THE EMC

by

F. W. Brasse

NOTKESTRASSE 85 · 2 HAMBURG 52

To be sure that your preprints are promptly included in the
HIGH ENERGY PHYSICS INDEX ,
send them to the following address (if possible by air mail) :

DESY
Bibliothek
Notkestrasse 85
2 Hamburg 52
Germany

DESY 82-047
July 1982

HADRONIC FINAL STATES IN HIGH ENERGY MUON-NUCLEON SCATTERING, RECENT RESULTS FROM THE EMC

F. W. Brasse

D E S Y
Hamburg

(Talk given at the Neutrino '82, the International Conference on Neutrino Physics, June 14-19, 1982, Balatonfüred, Hungary)

Abstract

Recent results on various aspects of hadronic final states in deep inelastic muon-nucleon scattering as obtained by the European Muon Collaboration (EMC) are presented and compared with QCD: the scaled energy distributions of charged hadrons, the average p_T^2 of neutral mesons and the azimuthal dependence of charged hadrons. The size of the primordial transverse momentum is being discussed in connection with the inclusion of soft gluons. Preliminary results for hadron production on nuclei are given. Finally the new experiment (NA9) of the EMC is briefly described.

Introduction

In the first phase of experiments carried out by the EMC the object was to study the scaling violation of the structure functions and, related to this talk, the production of hadrons in the fragmentation region of the electromagnetic current. For these experiments a forward spectrometer /1/ was used with an open dipolmagnet, with some identification of charged particles by a Cerenkov counter and in the late part of data taking with the inclusion of a lead glass detector to measure photons. High statistic results on F_2 (x, Q^2) /2,3,4/ have lead to a rather low QCD-scale breaking parameter Λ of around 150 MeV. Already the early results of the EMC on charged hadronic final states /5, 6, 7/, covering a kinematic range up to $W^2 \approx 450$ GeV^2 and $Q^2 \approx 100$ GeV^2, showed for the transverse momentum behaviour and the production of forward jets good agreement with predictions by QCD including nonperturbative effects. These results were complemented by the measurement of the yield of fast protons and antiprotons /8/, for which models are developped /9, 10, 11/. More recent results presented here add considerably to the understanding of the production of hadrons in the current fragmentation region.

For the second phase of experiments of the EMC a vertex detector, covering the target fragmentation region, and more particle identification were added to the forward spectrometer. Data taking commenced in fall 1981, and first results can be expected soon.

Scaled Energy Distributions of charged Hadrons

The distribution of the sum of positive and negative hadrons over the scaled energy $z = E_h/\nu$ (ν the energy of the virtual photon), normalized to N_μ, the number of events, has been studied /12/ as a function of Q^2, the square of the four momentum transfer by the virtual photon, of Bjorken $x = Q^2/2M\nu$ and of W^2, the square of the mass of the final hadronic system. In the quark parton model (QPM) this distribution is given for hadrons of type h by

$$\frac{1}{N_\mu}\left(\frac{dN^{h+}}{dz} + \frac{dN^{h-}}{dz}\right) = \sum_i \varepsilon_i(x)\left\{D_i^{h+}(z) + D_i^{h-}(z)\right\} \qquad (1)$$

with $\varepsilon_i = e_i^2 \cdot q_i(x) / \sum_j e_j^2 q_j(x)$, where the $q_i(x)$ are the quark distributions and i, j run over quarks and antiquarks of all flavours. $D_i^h(z)$ is the probability for a quark of type i to fragment into a hadron of type h. In the QPM (1) is independent of Q^2 and the factorisation structure of (1) leads, neglecting strange and charm quarks, to a complete independence of x for pions:

$$\frac{1}{N_\mu}\left(\frac{dN^{\pi+}}{dz} + \frac{dN^{\pi-}}{dz}\right) \approx D_u^{\pi+}(z) + D_u^{\pi-}(z)$$

Without any particle identification this is then equivalent to the distribution of all charged hadrons $(dN^+/dz + dN^-/dz)/N_\mu$, if one neglects differences for the fragmentation into strange mesons and baryons. In the leading logarithm approximation of QCD the ε_i and D_i^h become Q^2 dependent, but the factorization structure remains. However in 1. order of QCD, with the emission of gluons and their fragmentation into hadrons also, with the gluon vertex correction and with the q, $\bar{q}$ production coupled to the nucleon via a gluon,

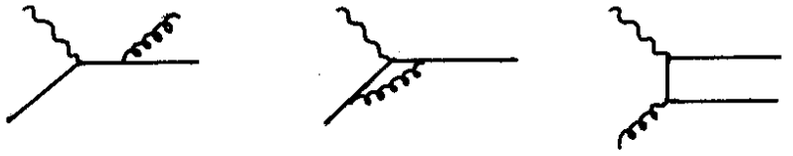

the expression $(dN^+/dz + dN^-/dz)/N_\mu$ becomes also x dependent /13/.

The data used for this analysis were taken with a primary energy of 280 (120) GeV on a 6 m long H_2 target, however interactions in the downstream 3m (2 m) part were selected only. Cuts were applied to the data to keep the systematic error on $(dN^+/dz + dN^-/dz)/N_\mu$ in all bins of z, Q^2 and x below 10 %. The remaining number of events are 35 K (25 K).

The Q^2 dependence of the resulting multiplicity is shown for two intervalls of x and for different z bins in Fig. 1 a. Especially at the higher values of z a small but definite decrease of the multiplicity with Q^2 is seen. The dashed curves are the result of a QPM calculation, based on standard quark distribution functions /14/, and fragmentation functions /15/, and show no Q^2 dependence. The full lines however, resulting from a 1. order QCD calculation /16/ with quark and gluon distributions from /17/, fragmentation functions from /18/ with Λ = 500 MeV, show a decrease with Q^2 in qualitative agreement with the data.

The x dependence, now for two fixed intervalls of Q^2, is given in Fig. 1 b, again together with the QPM and QCD calculations. The data show an increase of the multiplicity with increasing x. This behaviour is also represented by the QCD calculation.

A more quantitative picture of the amount of scaling violation and factorization breakdown is obtained by looking at the derivatives of $\ln((dN^+/dz + dN^-/dz)/N_\mu)$ with respect to $\ln Q^2$ and $\ln x$. These quantities are shown in Fig. 2 as a function of z for all available bins of x respectively Q^2 /19/. The full lines are the QCD calculation. Especially from these figures it is clear, that this QCD calculation represents the main trend of the data, but does not agree with them quantitatively. It should be noted however, that no attempt was made to vary the input: the quark and gluon distribution and fragmentation

functions. For the scale breaking parameter Λ one would expect it to be the same as for structure functions. It had been pointed out, that this QCD calculation does not treat the parton distributions in 1. order QCD, which should be done to obtain a more reliable result /20/.

Instead of choosing the variable Q^2 or x, one can use also W^2, the square of the total energy of the final hadrons in their center-of-mass system. At fixed values of W^2 the data do neither show a Q^2- nor a x-dependence. The data therefore were combined and Fig. 3 shows their W^2 dependence for the different z bins. A clear decrease of the multiplicity with increasing W^2 is observed for all values of z shown ($z > 0.15$), which is also present in the QCD calculation for $z > 0.25$. This result may indicate, that only the amount of energy being transfered to the struck quark is important for the amount of gluon radiation, leading to less and less particles of high momenta with increasing W^2. This effect has at least to be compensated at small values of z, apparently only below $z = 0.15$, by an increase of the multiplicity with increasing W^2. Because of the independence of x at fixed energy W the gluon radiation and the quark and gluon fragmentations seem to be roughly independent of the quark content of the nucleon.

Transverse Momentum of neutral Pions

Neutral pions have been measured using a leadglass detector, which was placed symmetrically around the beam in the forward spectrometer in front of the hadron absorber (see Fig. 13). It consisted of a preshower section with 5,5 radiation length of leadglass and two MPWC's, having ADC readout on cathode strips, and a back array of 450 leadglass blocks 8 x 8 x 40 cm^3 adding another 13,5 radiation length. This detector covers an area of 2.4 m vertically times 1.2 m horizontally.

Data were taken with 200 GeV primary muons on 6 m of H_2-target, but only events in the downstream 3 m were used. Showers were selected giving at least 5 GeV of total energy in the leadglass and at least 0.5 GeV in the back array. Neutral pions were separated from single photons by requiring two separated showers in the back array in the π^0 - energy range of 5 - 20 GeV, thus giving the energies of the two photons separately and their opening angle. In the range 20 - 80 GeV again either two separated showers were required (very asymmetric decays) or two separated clusters in the MWPC, thus giving the opening angle of the two photons in the almost symmetric decay and the combined energy. Above 80 GeV no π^0 are used. A Monte Carlo program was developped, which simulated production and detection of π^0's leading to a full agreement of the mass spectrum between data and Monte Carlo. At present 8500 π^0's are in the results. At least a factor of two more can be expected from more data being analysed.

In Fig. 4 the scaled energy distribution of π^0's is compared with those for hadrons of positive and negative charge, as measured by the EMC at 280 GeV. The neutral pions

are lying nearer to the negative hadrons than to the positive ones, which can be understood, as protons and kaons are not subtracted. For a quantitative comparison a large sample of identified $\pi^{\pm}$ is necessary which is not yet available at these energies.

The overall p_T^2 - distribution of π^{0}'s ($Q^2 > 3$ GeV^2, $50 \leq W^2 \leq 350$ GeV^2), where the p_T is measured with respect to the direction of the virtual photon, is shown in Fig. 5 and compared with a QCD calculation using the Lund model /21/. The main input parameters for the model are Λ = 500 MeV, fragmentation p_T of the primary quarks σ_q = 310 MeV and the primordial transverse momentum with $\langle k_T^2 \rangle$ = 0.65 GeV^2. The agreement of the model with the data is good. Excluding QCD effects and primordial k_T the high transverse momenta are clearly not reproduced.

Searching for the kinematic variation of the average p_T^2 of neutral pions Fig. 6 a shows the z^2, Fig. 6 b the Q^2 and Fig. 6 c and 6 d the W^2 dependence. In Figs. 6 a and 6 d the $\langle p_T^2 \rangle$ for charged hadrons is also shown and the agreement with the neutral pions is very good. Also given are the results from the Lund model using the same parameters as before. The agreement with the data as it had been for the $\langle p_T^2 \rangle$ of charged hadrons /5, 7/ is indeed good. The large amount of what is called primordial k_T needed is demonstrated in the z^2 distribution (Fig. 6 a), where $\langle k_T^2 \rangle$ = 0 in the model is also shown (dashed line). Eliminating in addition QCD (dashed dotted line) one sees only the transverse momentum resulting from fragmentation with a maximum of $\langle p_T^2 \rangle$ = 0.25 GeV^2 at z^2 = 0.3.

Azimuthal Distribution of charged Hadrons

To get more information about the primordial transverse momentum of the quarks inside the nucleon, the azimuthal distribution of charged hadrons has been studied. The azimuthal angle ϕ is measured between the scattering plane and the plane defined by the observed hadron and the virtual photon (Fig. 7). In general the dependence on ϕ can be written as follows, assuming single photon exchange:

$$\frac{1}{N_\mu} \cdot \frac{dN}{d\phi} = A + B\, f_1(y) \cos\phi + C\, f_2(y) \cos 2\phi + D \cdot P \cdot f_3(y) \sin\phi \qquad (2)$$

The f_i are known functions of the variable $y = \nu/E$ (E the energy of the primary muon), which is directly related to the polarisation of the virtual photon. P is the polarisation of the initial muon. The $\cos\phi$ term corresponds to the interference between longitudinal and transverse photons, the $\cos 2\phi$ term to transversely polarised photons and $\sin\phi$ to the polarisation of the initial lepton. In the QPM rather clean predicitions were made /22/, relating the $\cos\phi$ and $\cos 2\phi$ term to the initial transverse momentum k_T of the struck quark:

$$\langle \cos\phi \rangle = -2 \cdot \frac{\langle k_T \rangle}{\sqrt{Q^2}} f_1(y)$$

$$\langle \cos 2\phi \rangle = +2 \cdot \frac{\langle k_T^2 \rangle}{Q^2} f_2(y)$$

It was already pointed out /22/, that this is to be expected for the quarks after scattering, that for the final hadrons however the ϕ-distribution will be smeared out by the fragmentation. Also from QCD a small azimuthal dependence of the hadrons is expected /23/.

To study the azimuthal dependence the same 280 and 120 GeV data have been used as for the scaled energy distributions. Fig. 8 shows the angular distributions for four different bins of Q^2 in the total range from 5 to 100 GeV^2. It is clearly seen, that the distributions are not constant, a $\cos\phi$ term seems to dominate. The distributions have been fitted with equation (2) and the results are given in Fig. 9. The $\cos\phi$ - term is indeed dominant and negative as expected. At small Q^2 also the $\cos 2\phi$ - term is different from zero and positive, again as expected. A QCD calculation including the effect of the primordial k_T has been carried out by Kroll and König /24/. The result for $\langle \cos\phi \rangle$ and $\langle \cos 2\phi \rangle$ is also shown in Fig. 9. The main input parameters for the calculation are α_s (Q^2 = 20 GeV^2) = 0.34, $\langle k_T^2 \rangle$ = 0.6 GeV^2 and σ_q = 0.31 GeV. The main trend of the data with respect to $\langle \cos\phi \rangle$ is reproduced, the $1/\sqrt{Q^2}$ behaviour as expected from the above simple equation is suppressed by phase space effects at low Q^2 /24/. If the $\langle k_T^2 \rangle$ is set to zero in the calculation (dashed line), the $\langle \cos\phi \rangle$ is practically zero, indicating that the QCD effect on the level of the hadrons is very small. It was also possible to show with the model calculation, that the fragmentation reduces the size of $\langle \cos\phi \rangle$ by roughly a factor two at all Q^2, when going from the parton level to the level of the observed hadrons.

Soft Gluons

In all the present and previous /5, 7/ comparisons of transverse momentum phenomena on single particle distributions with models the primordial k_T has to be rather high ($\langle k_T^2 \rangle$ = .6 - .8 GeV^2) to get agreement with data. This goes together with a rather high value of the QCD parameter Λ of 500 MeV. When however selecting events with at least four charged forward hadrons ($p_{Lab} \geq 6$ GeV) /6, 7/ the $\langle k_T^2 \rangle$ was only around 0.4 GeV^2. This large and inconsistent value of $\langle k_T^2 \rangle$ has led Andersson et al. /25/ to a modification of their model. They have explicitly introduced soft gluons, which are emitted and reabsorbed by the quarks during the scattering process and which in this way give some additional transverse momentum to the struck quark. The energy of

these gluons is too low to create extra $q\bar{q}$ pairs. They essentially may correspond to those soft gluons which in the usual treatment in QCD are cut away because of the infrared singularities. The amount of soft gluons is also controlled by α_s and the authors/25/ have chosen it to be the same as for hard gluons. They have made a new comparison with the $\langle p_T^2 \rangle$ of charged hadrons from the 280 GeV EMC data. This is shown in Fig. 10, where $\langle p_T^2 \rangle$ is given as function of z^2. For the result of the new Lund model, somewhat arbitrarily $\langle k_T^2 \rangle$ was chosen to be 0.2 GeV^2 and Λ = 300 MeV. The agreement with the data is indeed rather good.

As this new Lund model can describe data using reasonably small values of $\langle k_T^2 \rangle$ the question arises, is there any difference between the primordial k_T of the quarks and the p_T introduced by soft gluons? The authors claim, that the part of transverse momentum of the struck quark, arising from soft gluons and being transfered to the leading hadron, should be compensated by hadrons produced in the central region of rapidity. In the case of primordial k_T however the compensation should take place in the target (backward) region. To be able to do a full test on this picture data with target fragments are needed. As however the forward spectrometer data include part of the central region the test has been made and the result is shown in Fig. 11. In the upper half the p_T of the charged trigger particle ($p_{Lab} \geq 6$ GeV), defined by $z > 0.5$, for all events with $Q^2 > 5$ GeV^2 and $100 \leq W^2 < 340$ GeV, normalised to the number of events, is shown as a function of the rapidity Y_{CMS}. Also preliminary data taken on a D_2 target at 280 GeV are used. In the lower part the transverse momentum component of all other charged particles ($p_{Lab} \geq 6$ GeV) opposite to the transverse momentum of the trigger particle is plotted as function of Y_{CMS}. The solid line is the QCD calculation with soft gluons, Λ = 300 MeV and $\langle k_T^2 \rangle$ = 0.2 GeV^2, whereas the dashed line is for no soft gluons and $\langle k_T^2 \rangle$ = 0.74 GeV^2. Although the agreement between the solid curve and the data is convincing the complete test including the target fragmentation has still to be seen. For the trigger particle there is practically no difference in the rapidity distributions of the two cases.

Hadron Production on Nuclear Targets

There are speculations in the literature /26/ that the study of hadron production on nuclear targets would give information about the space-time development of the quark fragmentation and possibly about the quark-nucleon scattering cross section. If one scatters on a large enough nucleus and if the fragmentation process of the struck quark starts only after a time $\tau \propto E_q/m^2$ (E_q and m are energy and mass of the quark), then an interaction of the quark with a nucleon could take place first. This could lead to a suppression of high energy hadrons ($z > 0.5$ or large rapidity) in heavy nuclei compared to light ones, to an increase of the multiplicity in the central region of rapidity and to an increase of the $\langle p_T^2 \rangle$. These ideas are supported in lepton scattering by some measurements done at SLAC /27/ with a 20.5 GeV electron beam on D_2, Be, C, Cu and Sn targets, where indeed up to 40 % lower multiplicity was found on Cu compared to C at $z > 0.5$ and $Q^2 > 1$ GeV^2. Even at $z = 0.3$ the difference is more than 20 %.

Although this type of experiment is still foreseen by the EMC using also the vertex system, a feasibility study was made with the forward spectrometer which has led to some preliminary results. Carbon (8.1 g/cm^3) and Copper (30.9 g/cm^3) were used as targets. The thickness was chosen such to be comparable in radiation length with 6 m of H_2 for reasons of electromagnetic background in the spectrometer. Also the absorbtion length was not too different from 3 m of H_2. The nuclear targets were split into 6 thin ones, being spread out over the place of the downstream 3 m of H_2 (D_2) target, to have similar acceptances. The primary energy of the muons was 200 GeV. The following cuts were applied to the data: $Q^2 > 4$ GeV^2, $x_{BJ} > 0.02$, $25 < W^2 < 290$ GeV^2, $0.07 < y < 0.85$, $p_{Had} > 6$ GeV, $\theta_{\mu'} > 25$ mrad. At present 6300 events are in the Cu sample (70 % of the data) and 3400 in the C one (30 %). The differential hadron multiplicities are compared with those as obtained on hydrogen in Fig. 12 a, b in terms of the rapidity Y_{CMS} and in Fig. 12 c, d in terms of p_T^2. The data are divided into two different regions of the energy ν of the virtual photon. From these preliminary data one can conclude that there are no large differences between the three different targets in the Y_{CMS}, p_T^2 and also in the z (not shown) distributions. For a more detailed comparison more statistics is needed, also comparison with D_2 and extension of the data to cover the full rapidity range.

The new EMC experimental Program with a Vertex Detector

The forward spectrometer has been complemented by a large vertex detector (Fig. 13) consisting of a superconducting magnet, a streamer chamber around the target and large angle track chambers. This will allow the track measurement of charged hadrons over almost 4π solid angle and close to the primary vertex with a good possibility to reconstruct also complicated events and secondary vertices in the streamer chamber. Furthermore many detectors for particle identification have been added to the EMC apparatus (Cerenkov and time-of-flight counters), to cover as much in momentum space as possible. Data taking and analysis has started in the fall of 1981.

The main physics aims are the study of

- Target (diquark) fragmentation,
- Fragmentation into identified hadrons,
- Correlations among identified particles, for example among baryons,
- Transverse momentum balance,

- Complete three jet events with its particle content,
- Production of charm and strangeness,
- Fragmentation in heavy nuclei,
- Shadowing.

The new detector system is a powerful tool to carry out these studies, and important results can be expected, if sufficient beam time and general support will be made available for these experiments.

References

/1/ EMC, O. C. Allkofer et al., Nucl. Instr. Meth. 179 (1981) 445
/2/ EMC, J. J. Aubert et al., Phys. Lett. 105B (1981) 315
/3/ EMC, J. J. Aubert et al., Phys. Lett. 105B (1981) 322
/4/ EMC, J. J. Aubert et al., CERN-EP/82-48, Phys. Lett. to be published
/5/ EMC, J. J. Aubert et al., Phys. Lett. 95B (1980) 306
/6/ EMC, J. J. Aubert et al., Phys. Lett. 100B (1981) 433
/7/ J. Gayler, DESY 81-063 (1981)
/8/ EMC, J. J. Aubert et al., Phys. Lett. 103B (1981) 388
/9/ B. Andersson et al., LU TP 81-6
/10/ G. Schierholz and M. Teper, DESY 81-41 (1981)
/11/ A. Bartl et al., UWThPh - 81 - 28 (1981)
/12/ EMC, J. J. Aubert et al., CERN-EP/82-47, Phys. Lett. to be published; W. Stockhausen, Thesis, Univ. of Wuppertal WUB DI 82-2
/13/ For references see /12/
/14/ R. McElhaney and S. F. Tuon, Phys. Rev. D8 (1973) 2267
/15/ L. M. Seghal, Proceedings of the 1977 International Symposium on Lepton and Photon Interactions, Hamburg (1977), p. 837
/16/ R. Baier and K. Fey, Z. Physik C, Particles and Fields 2 (1979) 339
/17/ M. Glück et al., DO-TH 80/13 (1980)
/18/ R. Baier et al., Z Physik C, Particles and Fields 2 (1979) 265
/19/ These results are taken from W. Stockhausen, Thesis, WUB DI 82-2. For a small difference of the data used see there.
/20/ R. Petronzio, private communication
/21/ B. Andersson et al., Z. Physik C 9 (1981) 233
/22/ R. N. Cahn, Phys. Lett. 78B (1978) 269
/23/ H. Georgi and H. D. Politzer, Phys. Rev. Lett. 40 (1978) 3
/24/ A. König and P. Kroll, Univ. Wuppertal, private communication
/25/ B. Andersson et al., LU TP 81-8 (1981)

/26/ N. N. Nikolaev, Z. Physik C 5 (1980) 291, CERN-TH 2792 (1979); A. Bialas and E. Bialas, FERMI-LAB-Pub-79/57-THY (1979)
/27/ L. S. Osborne et al., Phys. Rev. Lett. 40 (1978) 1624

Figure Captions

Fig. 1 a Q^2 dependence of $(dN^+/dz + dN^-/dz)/N_\mu$

Fig. 1 b x dependence of $(dN^+/dz + dN^-/dz)/N_\mu$

Fig. 2 Derivatives of $\ln((dN^+/dz + dN^-/dz)/N_\mu)$ with respect to $\ln Q^2$ and $\ln x$

Fig. 3 W^2 dependence of $(dN^+/dz + dN^-/dz)/N_\mu$

Fig. 4 dN/dz for π^0 compared with charged hadrons

Fig. 5 dN/dp_T^2 for π^0 compared with QCD (Λ = 500 MeV, $\langle k_T^2 \rangle$ = 0.65 GeV^2, σ_q=310 MeV)

Fig. 6 a-d z^2, Q^2 and W^2 dependence of $\langle p_T^2 \rangle$ for π^0 compared with charged hadrons and QCD (Λ = 500 MeV, $\langle k_T^2 \rangle$ = 0.65 GeV^2, σ_q = 310 MeV)

Fig. 7 Definition of the azimuthal angle ϕ

Fig. 8 Azimuthal angular distributions of charged hadrons

Fig. 9 $\langle \cos\phi \rangle$, $\langle \cos 2\phi \rangle$ and $\langle \sin\phi \rangle$ of charged hadrons compared with a QCD Model including effects of primordial k_T and fragmentation

Fig. 10 $\langle p_T^2 \rangle$ vs. z^2 for charged hadrons compared with QCD including soft gluons (V); The different contribution are (I) from fragmentation, (II) QCD 1. order, (III) primordial k_T, (IV) soft gluons

Fig. 11 The rapidity distribution of the p_T per event of a charged trigger hadron ($z > 0.5$) (upper half) and of the balancing p_T of the other charged hadrons (lower half) compared with QCD with (——) and without (- -) soft gluons, but large k_T

Fig. 12 a,b Rapidity distribution of charged hadrons on H_2, C, Cu

Fig. 12 c,d p_T^2 distribution of charged hadrons on H_2, C, Cu

Fig. 13 The EMC (NA9) detector.

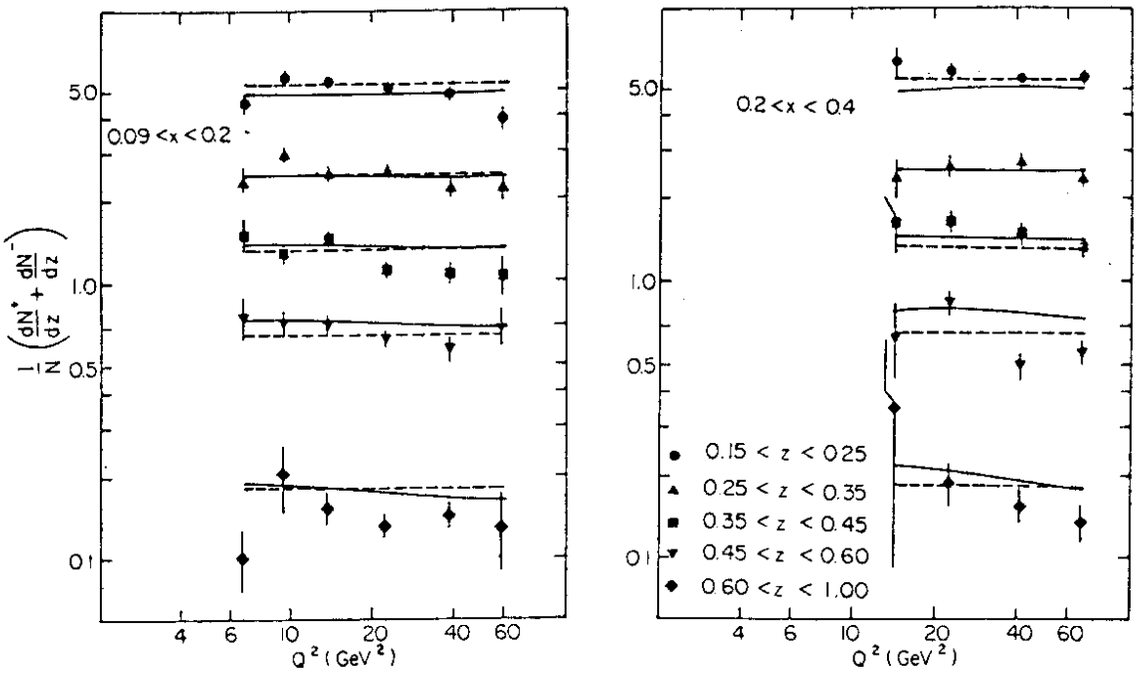
0.09 < x < 0.2
0.2 < x < 0.4
0.15 < z < 0.25
0.25 < z < 0.35
0.35 < z < 0.45
0.45 < z < 0.60
0.60 < z < 1.00
Q² (GeV²)

Fig. 1a

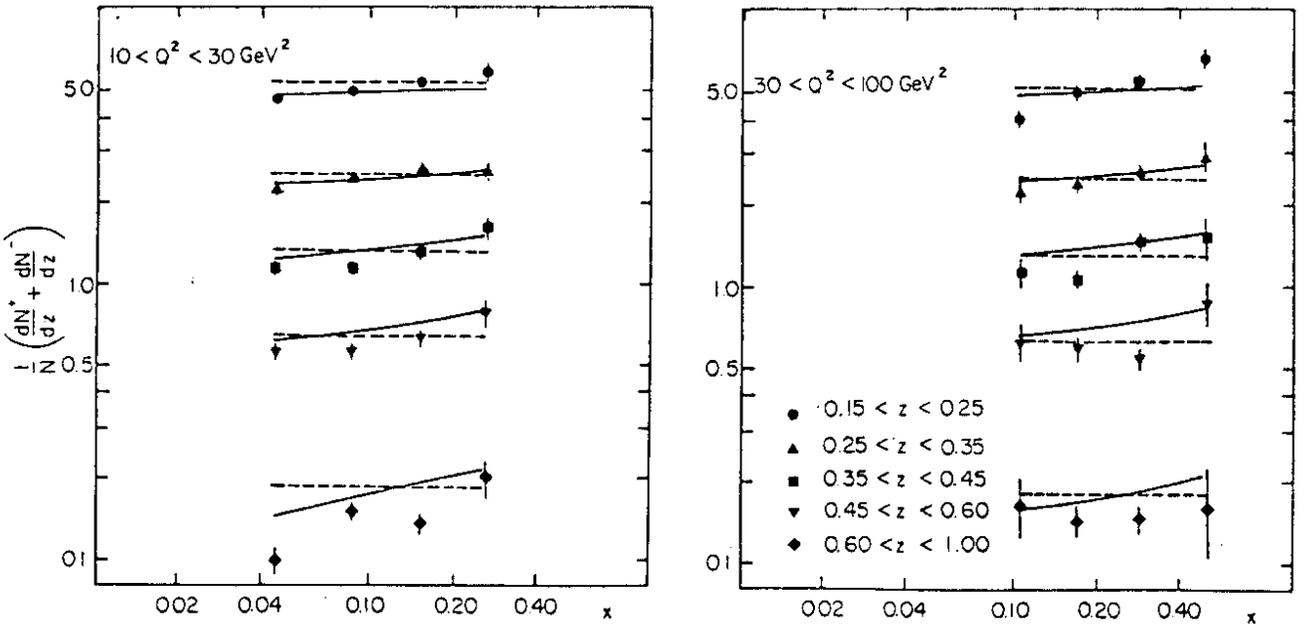
10 < Q² < 30 GeV²
30 < Q² < 100 GeV²
0.15 < z < 0.25
0.25 < z < 0.35
0.35 < z < 0.45
0.45 < z < 0.60
0.60 < z < 1.00
x

Fig. 1b

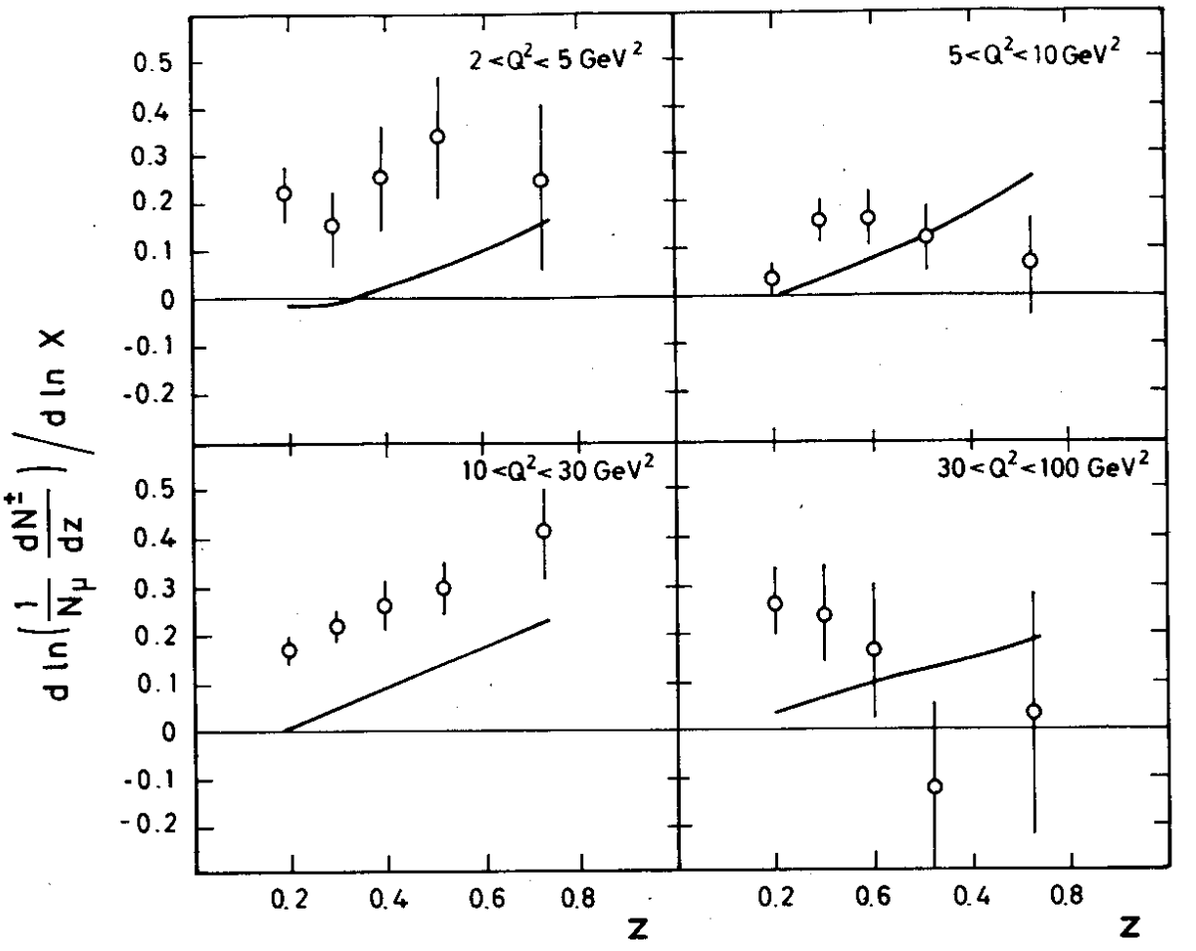
$2<Q^2<5\ GeV^2$
$5<Q^2<10\ GeV^2$
$10<Q^2<30\ GeV^2$
$30<Q^2<100\ GeV^2$
$d\ln\left(\frac{1}{N_\mu}\frac{dN^\pm}{dz}\right)/d\ln X$
z

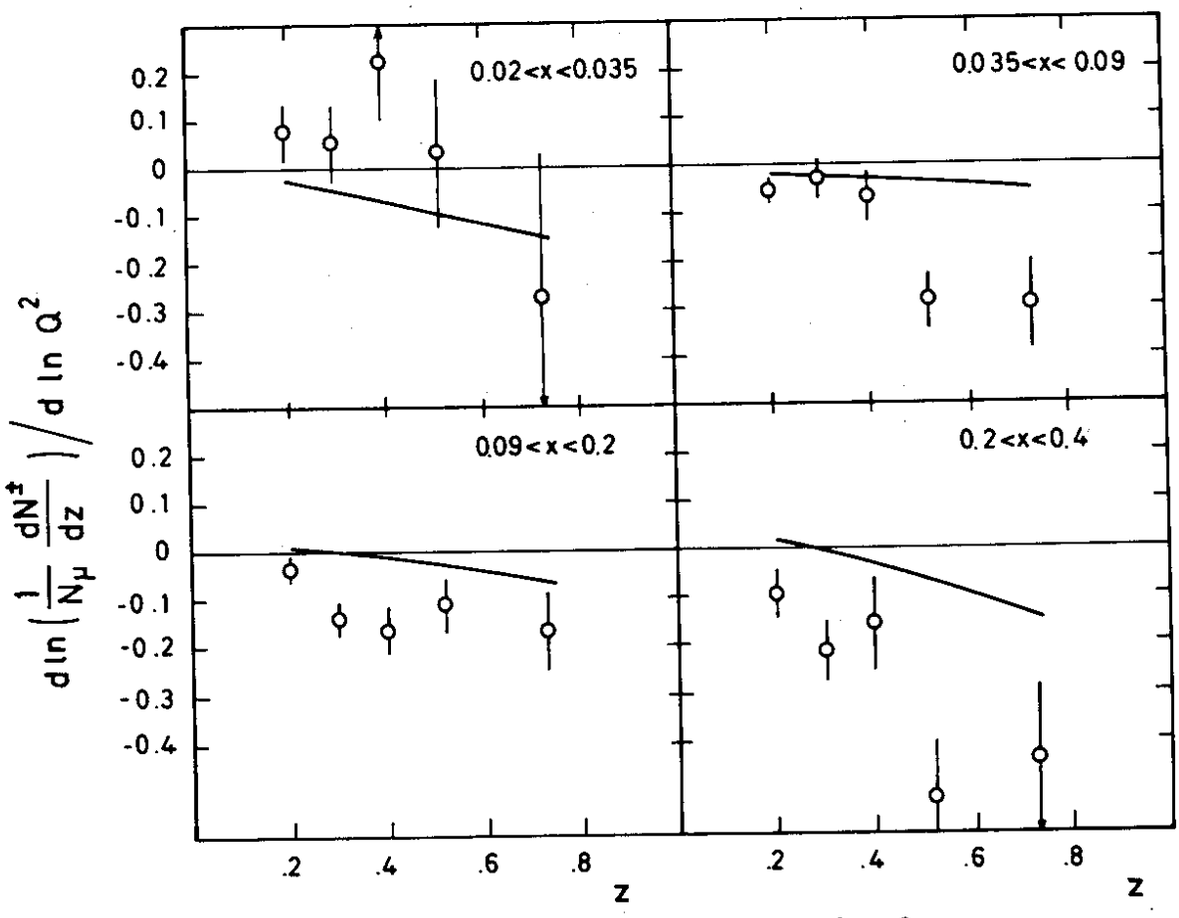
$0.02<x<0.035$
$0.035<x<0.09$
$0.09<x<0.2$
$0.2<x<0.4$
$d\ln\left(\frac{1}{N_\mu}\frac{dN^\pm}{dz}\right)/d\ln Q^2$
z

Fig. 2

34325

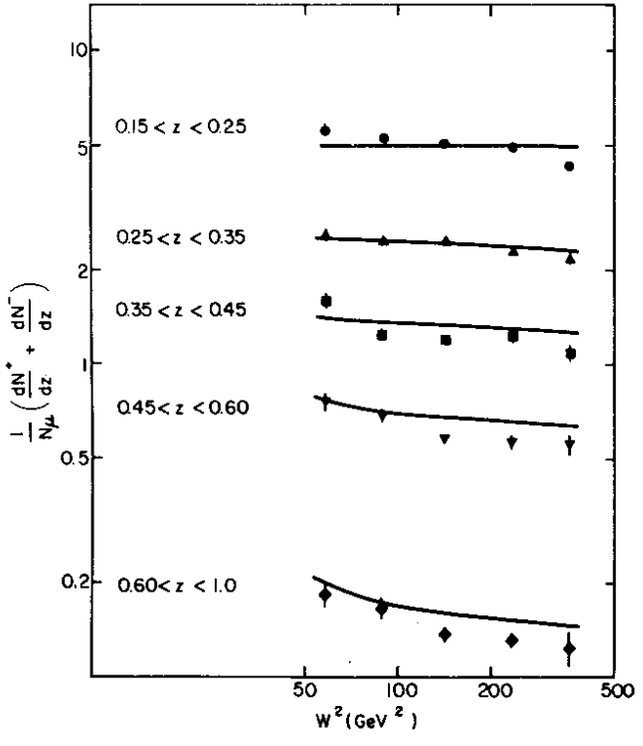

Fig. 3

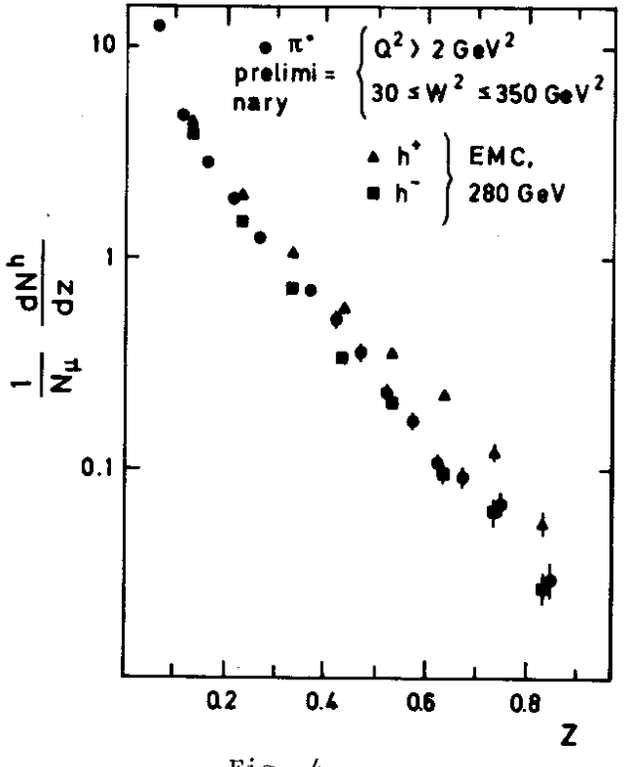

Fig. 4

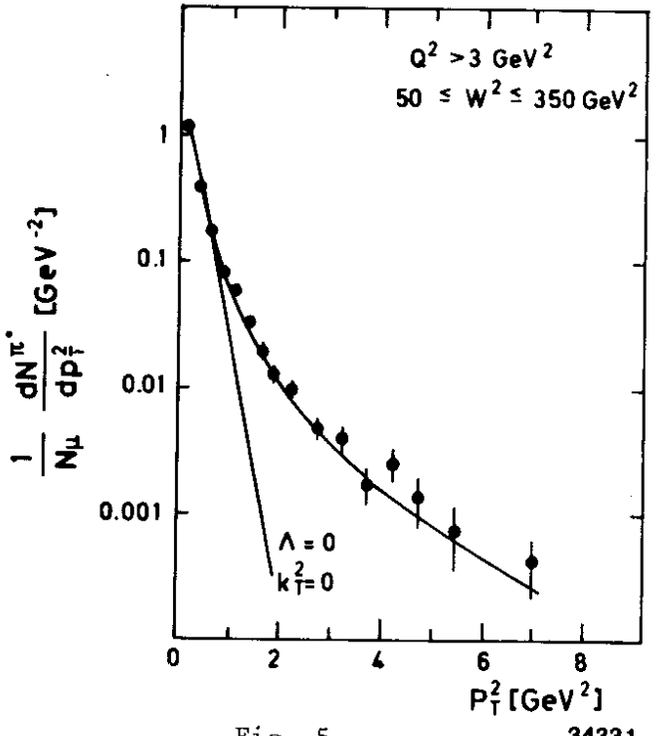

Fig. 5

34331

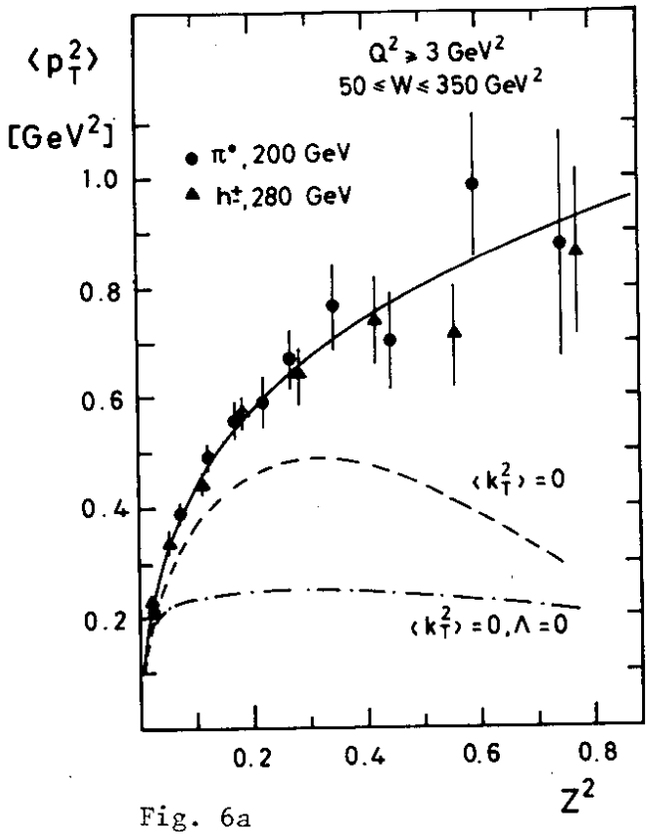

Fig. 6a

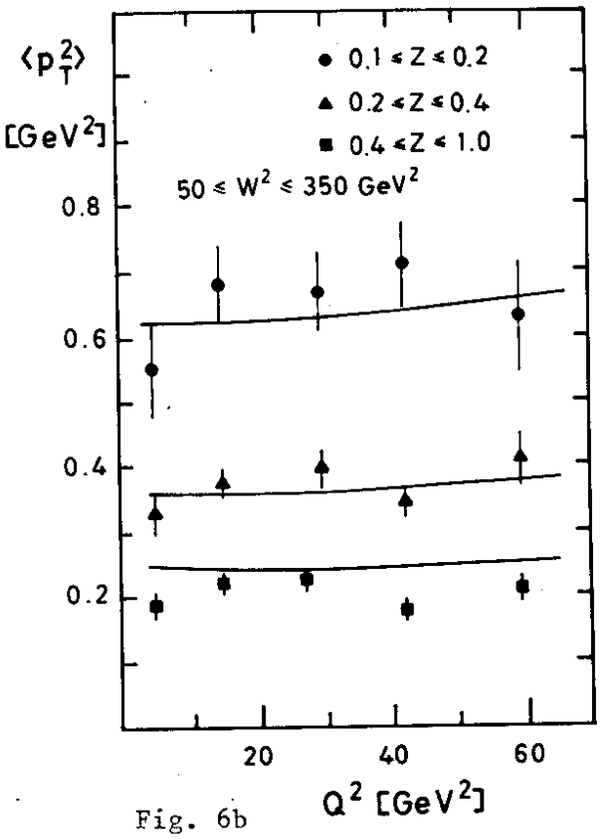

Fig. 6b

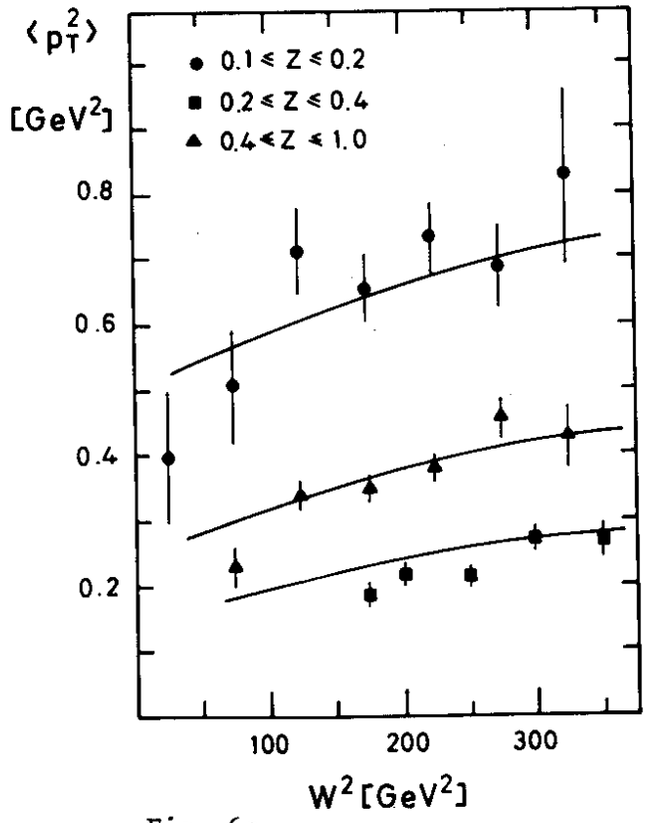

Fig. 6c

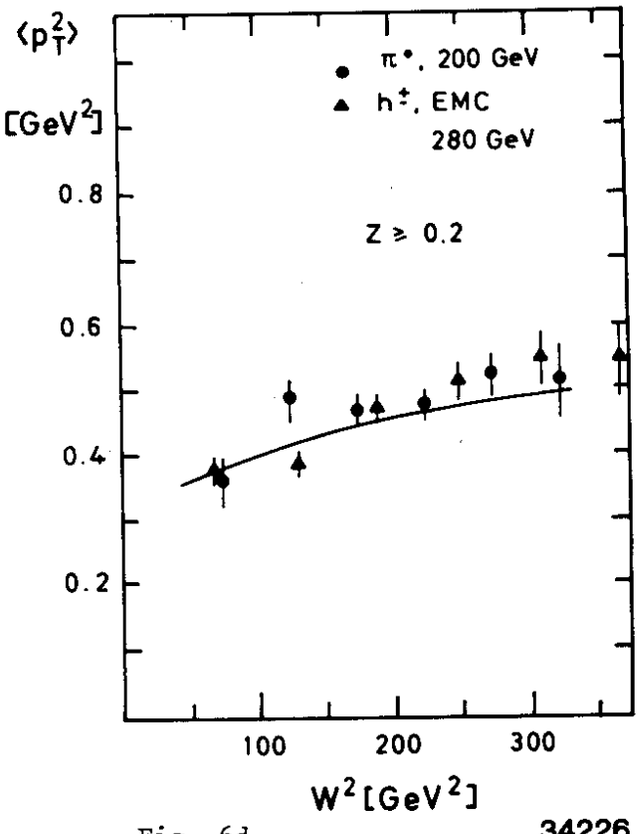

Fig. 6d

34226

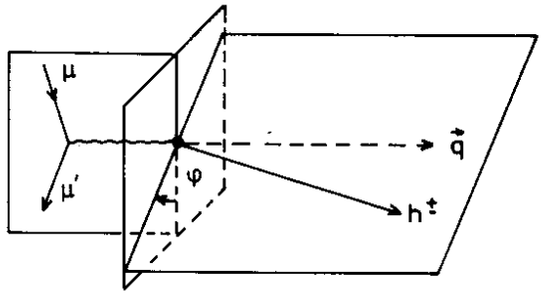

Fig. 7

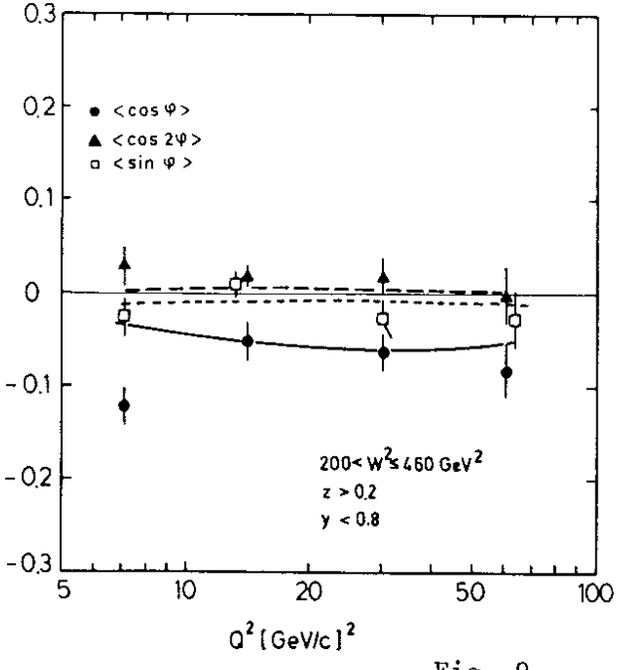

Fig. 9

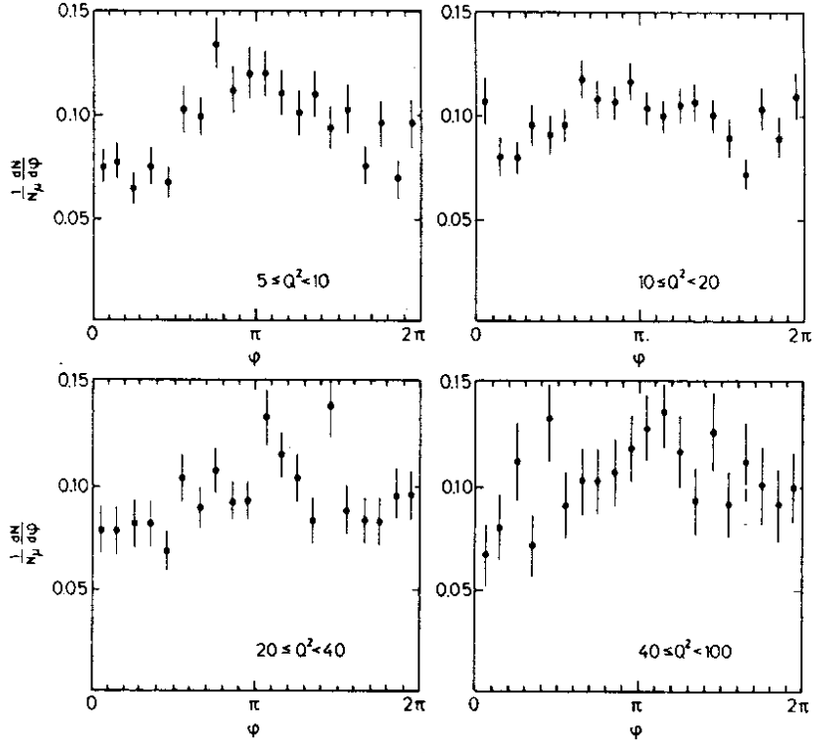

Fig. 8

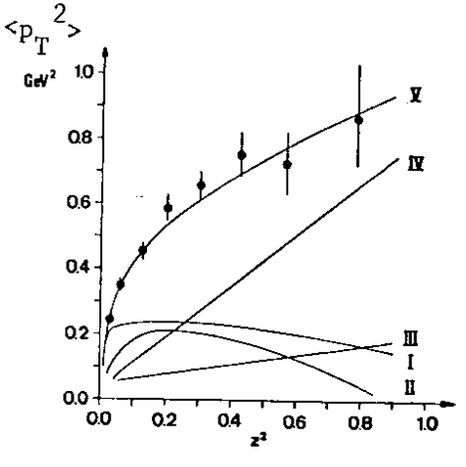

Fig. 10

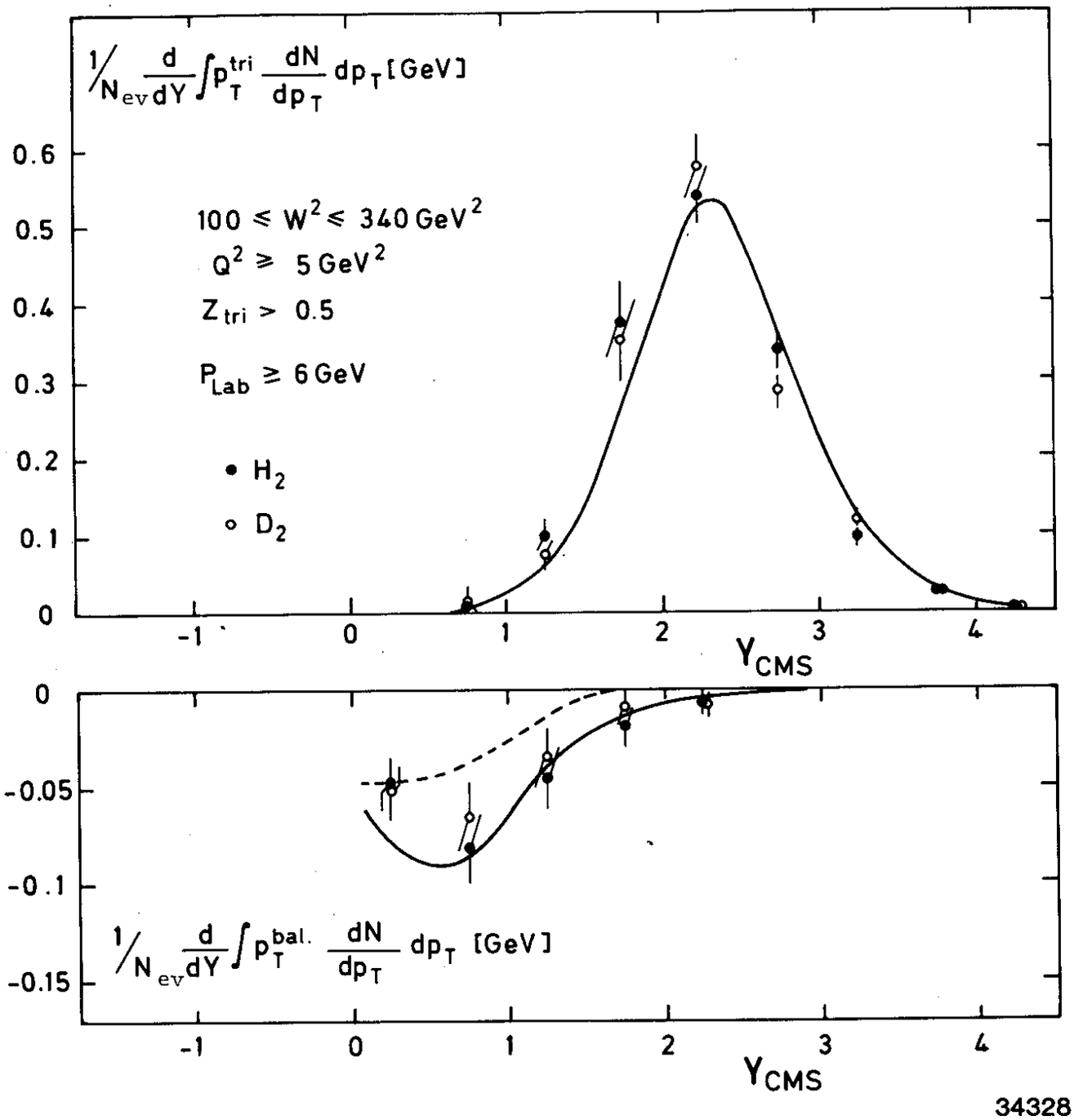
$\frac{1}{N_{ev}}\frac{d}{dY}\int p_T^{tri}\frac{dN}{dp_T}dp_T$ [GeV]
$100 \leq W^2 \leq 340\,GeV^2$
$Q^2 \geq 5\,GeV^2$
$Z_{tri} > 0.5$
$P_{Lab} \geq 6\,GeV$
• H_2
○ D_2
0.6
0.5
0.4
0.3
0.2
0.1
0
-1
0
1
2
3
4
Y_{CMS}
0
-0.05
-0.1
-0.15
$\frac{1}{N_{ev}}\frac{d}{dY}\int p_T^{bal.}\frac{dN}{dp_T}dp_T$ [GeV]
-1
0
1
2
3
4
Y_{CMS}
34328

Fig. 11

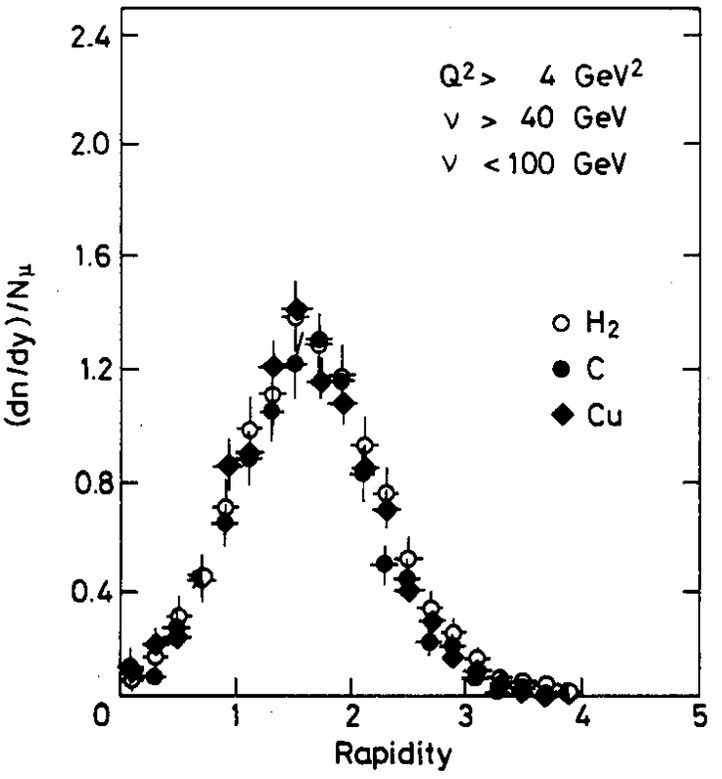

Fig. 12a

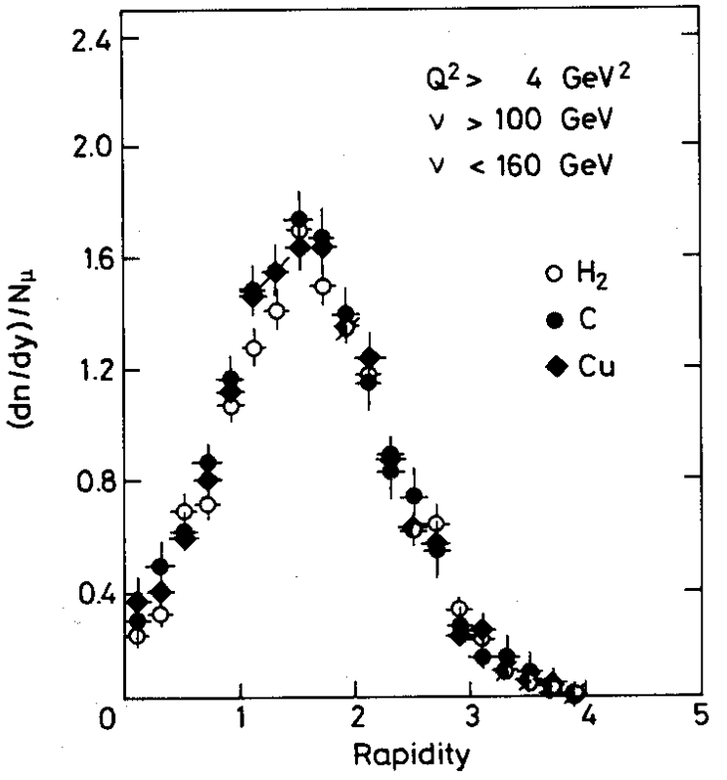

Fig. 12b

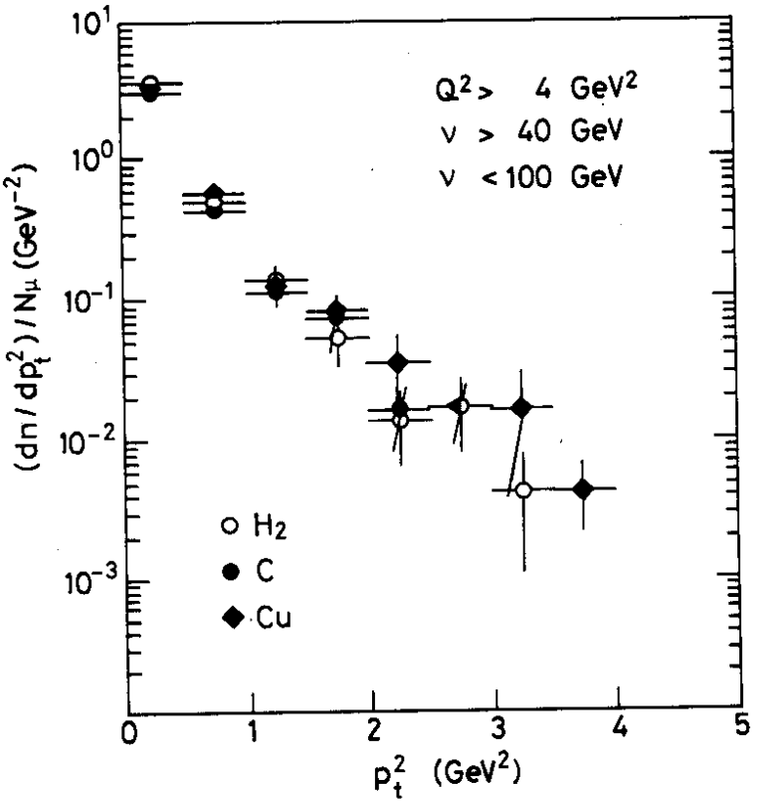

Fig. 12c

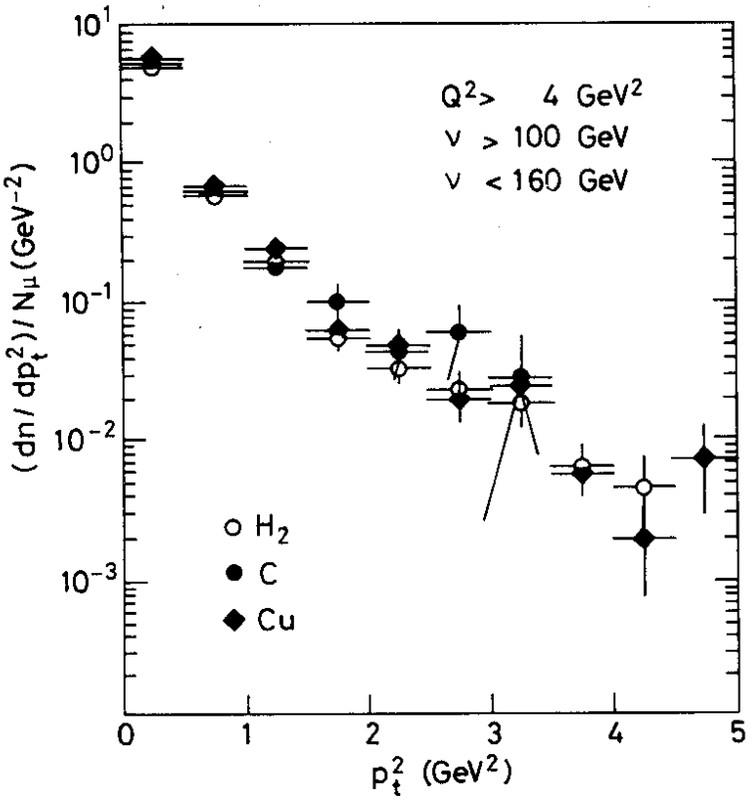

Fig. 12d

EMC (NA 9) - DETECTOR

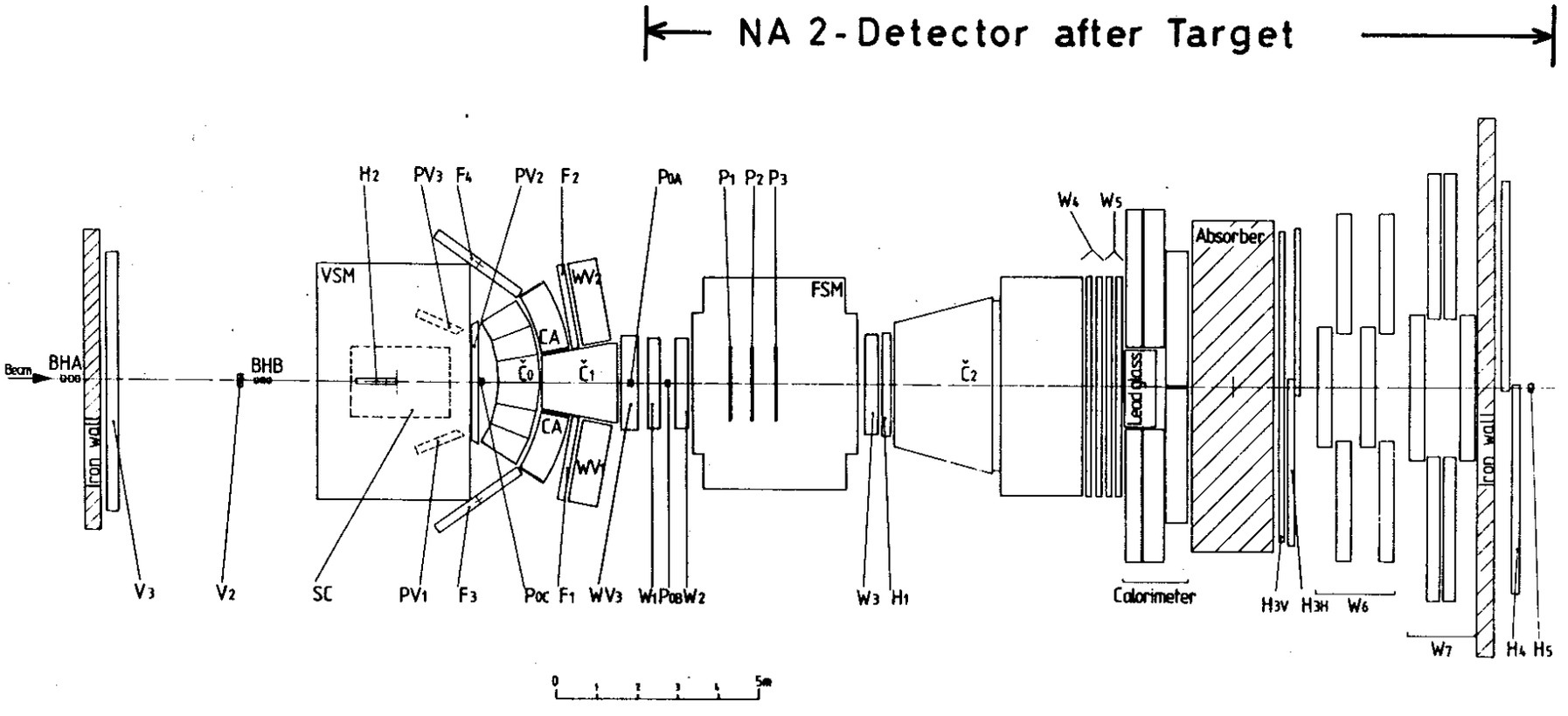

VSM = Vertex Magnet; FSM = Forward Magnet; SC = Streamer Chamber; PV1-3, P1-3, POA-C = Prop. Chambers; W1-7 = Driftchambers; H1-5, F1-4, BHA-B = Hodoscopes; V2-3 = Vetocounters; C0-2, CA = Cerenkovcounters

Fig. 13

34323